ISSN 2176-5480

22nd International Congress of Mechanical Engineering (COBEM 2013)
November 3-7, 2013, Ribeirão Preto, SP, Brazil

THERMAL ANALYSIS OF AN AERONAUTICAL PITOT PROBE WITH ANTI-ICING SYSTEM: MODELING, SIMULATION AND PARAMETRIC STUDIES

Kleber Marques Lisbôa
José Roberto Brito de Souza
Renato Machado Cotta
Laboratório de Transmissão e Tecnologia do Calor – LTTC, POLI & COPPE/UFRJ, Rio de Janeiro, RJ
kleberlisboa@poli.ufrj.br
jr.bs1959@gmail.com
cotta@mecanica.coppe.ufrj.br

Abstract. *This work proposes a conjugated heat transfer model for the thermal analysis of a heated aeronautical Pitot tube in combination with a robust hybrid numerical-analytical solution methodology. The energy equation for the solid is simplified by reformulating the radial diffusion term using the Coupled Integral Equations Approach – CIEA, obtaining in this way a transient one dimensional model for the transversally averaged temperature of the Pitot tube, which is then solved via the Generalized Integral Transform Technique – GITT. As for the fluid flow and energy equations, they are solved using the integral method along with the Crocco-Busemann relation. These governing equations are then handled through an iterative process responsible for the coupling of the temperature fields within the two regions. The model and the simulation routine developed in the Mathematica 7 platform are then validated with available experimental data for both incompressible flow wind tunnel runs and compressible flow A4 Skyhawk flights. The conducted parametric analysis suggests a few modifications in the sensor for improved anti-icing performance, such as employing a higher power density near the stagnation point for a fixed total power and the use of a straight cylindrical probe instead of a cylinder-cone configuration.*

Keywords: *Pitot probe, Anti-icing, Conjugated problem, Integral transforms, Integral method*

1. INTRODUCTION

Icing of aeronautical surfaces and the consequent degradation in flight performance under high altitude and adverse atmospheric conditions is a well known and studied phenomenon since World War II. The main affected parts are the wings, empennages, engine intakes, frontal cone, landing gear compartment's door and sensors (GENT et al., 2000; CALISKAN et al., 2008). Among these, the case of the Pitot tube is emphasized in this work since it is still a fundamental equipment for guidance and navigation of modern aeronautical systems. The icing of such probes can generate unreliable local velocity readings and compromise the flight control. The catastrophic effects of this kind of failure can be observed when analyzing the recent accident occurred with the AF447 flight in 2009, in which the Pitot probes icing, complicated by deficient crew training in high altitude flights with abrupt loss of lift, was pointed out as the main cause of the disaster by the investigations conducted by the Bureau d'Enquêtes et d'Analyses pour la Sécurité de l'Aviation Civile (BEA), France. However, this was not the only accident in which the icing of the sensors were pointed as the main cause of an aeronautical disaster. In a brief survey conducted, a few other cases were found with very similar circumstances as that of the AF447, showing the importance of pursuing further analysis on the subject.

A substantial amount of information and studies about wing, empennage and engine intakes icing can be readily found in the open literature, in light of the commercial and strategic advantages that such knowledge can provide. Controlled distribution software were developed throughout recent years, such as LEWICE, ONERA2D, TRAJICE, CANICE and many others. Even though the importance of studying the icing of Pitot tubes is well recognized for the reasons already discussed, very little information concerning this particular subject was found in the open literature, possibly due to commercial issues or to a minimized importance in comparison with icing problems on other more vital aircraft components. Having the aerial transportation user well being in mind, it is important that such analysis be undertaken and the information be available in order to question project decisions and confront the manufacturer adequately when failures occur.

In a large number of situations involving convective heat transfer in thermal engineering, it is fairly usual to simplify the mathematical formulations ignoring the influence of the heat transfer process within the solid wall on the fluid temperature field or vice versa, in both external and internal convection. For this reason, in most applications, empirical correlations for the heat transfer coefficient obtained under prescribed boundary conditions – usually constant heat flux or temperature – are used to estimate heat transfer rates by natural, forced or mixed convection. This is mainly due to the unavailability of heat transfer coefficients correlations for all possible boundary conditions and configurations combinations, and the use of this approach can be credited to the simplification it implies in the mathematical model to be solved. On the other hand, there is always the alternative of employing more involved models

ISSN 2176-5480

in the form of conjugated conduction-convection problems, when accuracy is at a premium. However this option adds significant mathematical complexity to the problem formulation, since it often requires the solution of the fluid flow equations together with the coupled thermal energy balances both in the fluid and in the solid, rendering a very difficult problem to solve even numerically. Aeronautical thermal protection systems are designed so that the solid be capable of rapidly responding to the external convection stimulus, due to sudden variations of atmospheric conditions, being thus essential to solve the conjugated conduction-convection in such cases, a notion that will be recalled along this text. Ignoring this mutual influence could lead to erroneous results and physical conclusions that could induce the designer of such equipment to make wrong decisions.

This contribution is an extension of previous efforts within the same research group. The first work (Souza et al., 2011) comprises the proposition of a plain radially lumped formulation for the Pitot probe with the use of correlations for the required external heat transfer coefficients, then validated with experimental wind tunnel runs within the incompressible flow range. The second work (Souza et al., 2012) reports experimental results of the A4 Skyhawk flights with an instrumented Pitot tube, subjected to planned thermal transients, within the compressible flow regime. A conjugated problem analysis is then introduced, with an approximate local similarity solution being adopted for the external flow problem, which is then critically compared to the previously proposed simplified formulation (Souza et al., 2011), with the aid of the experimental temperature measurements from the A4 flight tests. In this context, the present work has the objective of further advancing the analytical tools for understanding anti-icing systems for aeronautical velocity sensors, through the proposition of the inherently required conjugated conduction-convection problem and a robust hybrid numerical-analytical solution methodology. The analysis of the thermal behavior that precedes the onset of ice formation can be used to modify the probe design, aimed at avoiding the freezing of the impinging supercooled droplets or ice crystals in flights under adverse atmospheric conditions.

2. PROBLEM FORMULATION

In light of the opportunity offered by the Brazilian Navy in performing tests with their A-4 Skyhawk aircrafts, the Pitot tube shown in Figures 1 and 2, which is mounted on the A-4, was used as the basis for the modeling here developed, having essentially the same characteristics of more modern velocity probes. It is important to mention that the Pitot tube in consideration is equipped with an anti-icing thermal protection system located in the central cylindrical part of its body, which consists of a resistive metallic wire embedded in a ceramic electrical insulation. From the stagnation region at the conical tip until close to the leading edge of the support, which resembles a wing, where the heated region ends, the material used is copper, while the rest is made of brass. The exception is the electrical insulation present in the heated region that is composed of porcelain which will be the subject of further discussions in what follows. The detailed knowledge of the flow and heat transfer processes over and within the probe itself is essential for its thermal management, specially near the stagnation region due to its functional importance, while the support region, holds little importance to the thermal behavior of the sensor as a whole (Souza et al., 2011).

Figure 1. Pitot probe PH-510 used as the basis for the proposed thermal model.

Figure 2. Pitot probe PH-510 mounted on the A4 Skyhawk aircraft of the Brazilian Navy, São Pedro d´Aldeia Naval Base.

Aiming at developing a thermal model for the Pitot probe with anti-icing system, two physical regions are considered. The first one is the solid shell that comprises the body of the sensor which is modeled through the heat conduction equation with an energy generation term, due to the anti-icing heating. The other region is related to the mechanical and thermal boundary layers that are formed around the axisymmetric shape of the sensor as depicted in general form in figure 3 below. The boundary layers are then split in two portions, laminar and turbulent, that are

ISSN 2176-5480

treated separately and with a sharp transition when the critical Reynolds number is reached. The flow external to the boundary layer is also required, where the influence of the viscosity is not relevant and an inviscid model can be invoked. Moreover, there are analytical relations for the potential flow over an axisymmetric body that are readily available from aerodynamics textbooks, due to its importance in calculations of fuselage bodies. With the velocity field and making the assumption that the flow is isentropic, the temperature, density and dynamical viscosity fields, using the Sutherland relation, easily follow (White (1992), Kays & Crawford (1980), Cebeci & Cousteix (2005), Schlichting (1979)). The relations chosen in the present work are derived from Schlichting & Truckenbrodt (1979), which is based on sources and sinks distributions to establish the velocity fields at the border of the boundary layer, a common approach in potential flow theory. However, the originally proposed equations apply strictly only to incompressible flows. However, correction factors were developed along this period in order to take advantage of the simplicity of such results. Here, the Prandtl-Glauert correction is adopted since, even though there are more accurate factors, it is explicit, straightforward, and sufficiently precise for our purposes. The interaction between the solid and fluid regions occurs through the continuity relations for the temperature field and heat flux at the solid-fluid interface.

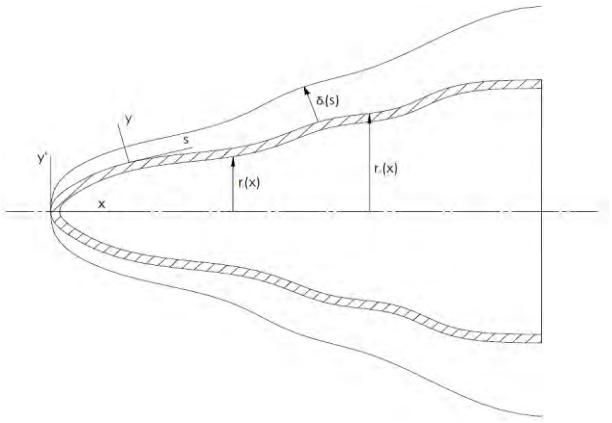

Figure 3. Coordinates system for the axissymetrical configuration of a Pitot tube with arbitrary geometry and its interaction with the external boundary layer

The geometrical complexity of the probe apparently poses difficulties in formulating a simplified model to the whole extension of the Pitot tube. However, a detailed local reproduction of the temperature field at the wing shaped support of the probe is not relevant, as observed in previous works (Souza et al., 2011; Souza et al., 2012), which allows simplification of the curvature effects in the transition from the conical-cylindrical portion towards the junction with the support. The mathematical model for heat conduction along the considered axisymmetric Pitot tube is presented in equations (1.a-f), employing cylindrical coordinates.

$$w(x,r)\frac{\partial T_s}{\partial t} = \frac{\partial}{\partial x}\left(k(x,r)\frac{\partial T_s}{\partial x}\right) + \frac{1}{r}\frac{\partial}{\partial r}\left(k(x,r)r\frac{\partial T_s}{\partial r}\right) + g(x,r,t), \qquad 0 \le x \le L,\ r_i(x) \le r \le r_o(x) \tag{1.a}$$

$$T_s(x,r,0) = T_0(x,r) \tag{1.b}$$

$$h_e T_s(0,r,t) - k(0,r)\frac{\partial T_s}{\partial x}\Big|_{x=0} = h_e T_{aw}; \quad \frac{\partial T_s}{\partial x}\Big|_{x=L} = 0 \tag{1.c,d}$$

$$\frac{\partial T_s}{\partial \boldsymbol{n}}\Big|_{r=r_i(x)} = 0; \quad h(x)T_s(x,r_o(x),t) + k(x)\frac{\partial T_s}{\partial \boldsymbol{n}}\Big|_{r=r_o(x)} = h(x)T_{aw} \tag{1.e,f}$$

In the above formulation, heat transfer from the probe support to the airplane structure is neglected, due to the minor importance of this region in the desired thermal analysis (Souza et al., 2011). Also, Newton's law of cooling at the boundary conditions is written for a more general conjugated problem with compressible flow, and for this reason the adiabatic wall temperature becomes important to the proposition of a model applicable in the whole envelope of applications desired.

Knowing that metallic materials are predominant in the sensor structure and that the wall thicknesses are in general small, it is expected that the Biot numbers are sufficiently low allowing for the application of a lumping procedure in the radial direction, towards the simplification of the solid heat conduction model. Both the classical lumped and the improved lumped approaches (Cotta & Mikhailov, 1997) are considered in the present text and a comparison between the two approaches shall be conducted in the following sections. The so called Coupled Integral Equations Approach (CIEA) for reformulation of differential problems is based on the proposition of approximations for both the averaged potential and its gradient as a function of the average potential, as defined through the integration in one or more spatial variables. For our specific problem, the radially averaged temperature is defined as:

ISSN 2176-5480

$$T_{av}(x,t) = \frac{2}{{r_o}^2 - {r_i}^2} \int_{r_i(x)}^{r_o(x)} T_s(x,r,t) r dr \tag{2}$$

Applying the same averaging operator in the differential model under analysis, it is possible to make use of Hermite approximations for numerical integration and to reformulate the transient two-dimensional model (1.a-f) into a transient one-dimensional model (Cotta & Mikhailov, 1997). Thus, applying the averaging operator in the radial direction to equation (1.a), using the definition of the radially averaged temperature, equation (2), and considering that the variation of the transversal section area with the longitudinal direction is mild, so as to approximate the normal derivatives by radial ones, it is possible to write the partial differential model of equations (1.a-f) as:

$$w_{av}(x)\frac{\partial T_{av}}{\partial t} = \frac{1}{A(x)}\frac{\partial}{\partial x}\left(k_{av}(x)A(x)\frac{\partial T_{av}}{\partial x}\right) + \frac{2k_{av}(x)r_o}{{r_o}^2 - {r_i}^2}\left.\frac{\partial T_s}{\partial r}\right|_{r=r_o(x)} + g_{av}(x,t), \quad 0 \le x \le L \tag{3.a}$$

$$T_{av}(x,0) = T_{av_0}(x) \tag{3.b}$$

$$h_e T_{av}(0,t) - k_{av}(0)\left.\frac{\partial T_{av}}{\partial x}\right|_{x=0} = h_e T_{aw}; \qquad \left.\frac{\partial T_{av}}{\partial x}\right|_{x=L} = 0 \tag{3.c,d}$$

Using Hermite approximations to numerically integrate equation (2) and the known integral of the gradient over the domain, together with the boundary conditions in the radial direction, it is possible to relate the local term in eq.(3.a) that is evaluated at the surface of the probe, with the average temperature, which results in equations (4.a-c), consisting of the so called improved lumped approach.

$$T_s(x,r_i,t) = \frac{12k_{av}(x)(r_o+r_i)T_{av}(x,t) + h(x)(r_o-r_i)[6(r_o+r_i)T_{av}(x,t) - (3r_o+r_i)T_{aw}]}{12k_{av}(x)(r_o+r_i) + h(x)(3r_o+5r_i)(r_o-r_i)} \tag{4.a}$$

$$T_s(x,r_o,t) = T_{aw} + \frac{12k_{av}(x)(r_o+r_i)(T_{av}(x,t) - T_{aw})}{12k_{av}(x)(r_o+r_i) + h(x)(3r_o+5r_i)(r_o-r_i)} \tag{4.b}$$

$$\left.\frac{\partial T_s}{\partial r}\right|_{r=r_o(x)} = -\frac{12h(x)(r_o+r_i)(T_{av}(x,t) - T_{aw})}{12k_{av}(x)(r_o+r_i) + h(x)(3r_o+5r_i)(r_o-r_i)} \tag{4.c}$$

As for the classical lumped analysis, the temperature of the surface is simply approximated by the average temperature in the boundary condition (1.f), also allowing for the association of the local term in the right hand side of equation (3.a) with the average temperature. In this case, the local temperatures at the internal and external surfaces of the probe, and the boundary condition at the external surface, are approximated as in equations (5.a-c):

$$T_s(x,r_o,t) \cong T_s(x,r_i,t) \cong T_{av}(x,t) \tag{5.a,b}$$

$$\left.\frac{\partial T_s}{\partial r}\right|_{r=r_o(x)} \cong \frac{h(x)}{k_{av}(x)}\left(T_{aw} - T_{av}(x,t)\right) \tag{5.c}$$

Eqs.(4.a-c) are in fact directly applicable only to the axisymmetric portion of the Pitot probe, within $0 \le x \le a$. However, for the wing-like support the use of the classical lumped approach is more easily applicable and sufficiently accurate for the present purposes. Therefore, as discussed above, neglecting the curvature effects on heat transfer to the support region, the complete improved lumped model for the Pitot probe becomes:

$$w_{av}(x)\frac{\partial T_{av}}{\partial t} = \frac{1}{A(x)}\frac{\partial}{\partial x}\left(k_{av}(x)A(x)\frac{\partial T_{av}}{\partial x}\right) - \Omega(x)(T_{av}(x,t) - T_{aw}) + g_{av}(x,t) \tag{6.a}$$

$$\text{where, } \Omega(x) = \begin{cases} \dfrac{24h(x)k_{av}(x)r_o}{12k_{av}(x)({r_o}^2 - {r_i}^2) + h(x)(r_o-r_i)^2(3r_o+5r_i)}, & 0 \le x \le a \\ \dfrac{h(x)P(x)}{A(x)}, & a \le x \le L \end{cases} \tag{6.b}$$

$$T_{av}(x,0) = T_{av_0}(x) \tag{6.c}$$

$$h_e T_{av}(0,t) - k_{av}(0)\left.\frac{\partial T_{av}}{\partial x}\right|_{x=0} = h_e T_{aw}; \qquad \left.\frac{\partial T_{av}}{\partial x}\right|_{x=L} = 0 \tag{6.d,e}$$

The relations used to transform into dimensionless form the above stated problem are presented in equations (7.a-e), while the result of its application is consolidated in equations (8.a-d):

$$X = \frac{x}{L};\ \tau = \frac{k_0 t}{w_0 L^2};\ k^* = \frac{k_{av}}{k_0};\ w^* = \frac{w_{av}}{w_0};\ \theta_{av} = \frac{T_{av} - T_{aw}}{T_{ref} - T_{aw}} \tag{7.a-e}$$

$$w^*(X)\frac{\partial \theta_{av}}{\partial \tau} = \frac{1}{A(X)}\frac{\partial}{\partial X}\left(k^*(X)A(X)\frac{\partial \theta_{av}}{\partial X}\right) - \frac{\Omega(X)L^2}{k_0}\theta_{av}(x,t) + \frac{g_{av}(X,\tau)L^2}{k_0(T_{ref} - T_{aw})} \tag{8.a}$$

$$\theta_{av}(X,0) = \frac{T_{av_0}(X) - T_{aw}}{T_{ref} - T_{aw}} \tag{8.b}$$

$$Bi_e\theta_{av}(0,\tau) - k^*(0)\left.\frac{\partial \theta_{av}}{\partial X}\right|_{X=0} = 0; \qquad \left.\frac{\partial \theta_{av}}{\partial X}\right|_{X=1} = 0 \tag{8.c,d}$$

ISSN 2176-5480

The probe materials and radial dimensions vary with the longitudinal direction and these changes in the effective thermophysical properties and transversal section are very important to the model response. Figures 4 and 5 display the dimensionless thermal capacity and the heat conductivity, respectively. It should be noted the sharp step in the thermal capacity at the end of the cone portion of the probe, that is 16 mm apart from the stagnation point. This is due to the large heat capacity of the ceramic material used to electrically insulate the resistance from the probe along the heated portion. It is also easy to observe that the influence of this ceramic material in the heat conductivity is less significant which was already expected, since it has thermal insulating properties. Careful dimensional measurements of the geometrical parameters were conducted in a damaged and opened PH-510 probe in order to determine the transversal section properties at each longitudinal station. The dimensionless results are presented in figures 6 and 7.

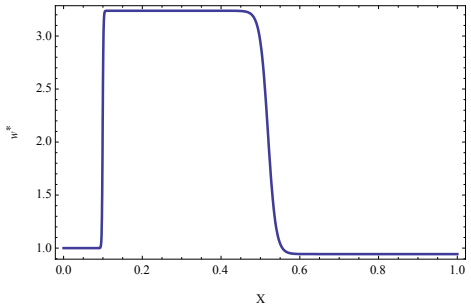

Figure 4. Spatial variation of the dimensionless heat capacity.

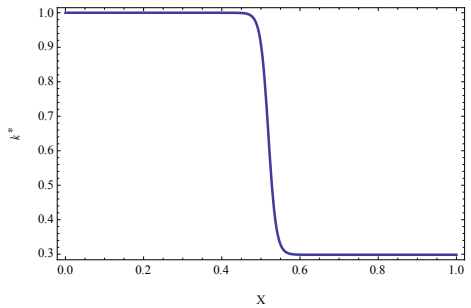

Figure 5. Spatial variation of the dimensionless heat conductivity.

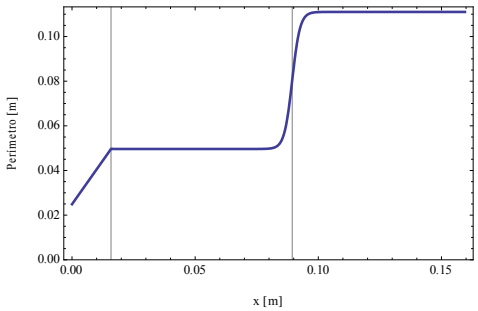

Figure 6. Dimensionless perimeter of the transversal section.

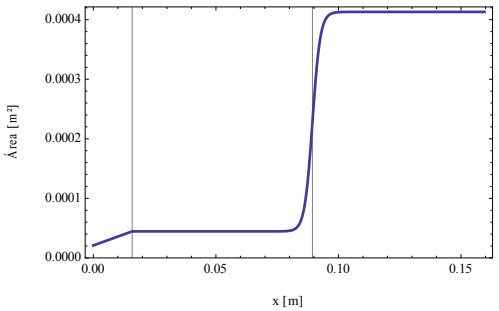

Figure 7. Dimensionless area of the transversal section.

The solution of the flow and energy equations in the fluid is carried only in the axisymmetric part of the Pitot tube allowing for the use of a specific coordinate system for this case in order to facilitate the solution even in irregular geometries. The flow is considered to be compressible since it is desired to cover all the flight envelope of modern commercial aircraft. As for the transient response, it was shown in a recent work by Lisboa et al. (2012) that the time necessary for the flow to reach steady state is at least 1000 times less than that necessary for the solid to reach the same regime. Therefore, only the quasi-steady state solution for the fluid will be considered here.

Within the limits of the boundary layer theory and from the assumptions that the fluid is Newtonian, that the Boussinesq postulate holds and that the turbulent Prandtl number is constant (Schlichting, 1979; White, 1992; Cebeci & Cousteix, 2005), equations (9.a-h) for the fluid flow problem are obtained. For the sake of brevity they are written in the form of Reynolds averaged equations. For laminar flow the turbulent properties are set to zero and the bars over the variables disappear.

$$\bar{\rho}\bar{u}\frac{\partial \bar{u}}{\partial s} + \overline{\rho v}\frac{\partial \bar{u}}{\partial y} = \rho_e u_e \frac{du_e}{ds} + \frac{1}{r}\frac{\partial}{\partial y}\left[(\mu + \mu_t) r \frac{\partial u}{\partial y}\right] \tag{9.a}$$

$$\bar{u}(0) = 0, \quad \bar{u}(\infty) = u_e, \quad \left.\frac{\partial \bar{u}}{\partial y}\right|_{y=\infty} = 0 \tag{9.b-d}$$

$$\bar{\rho}\bar{u}\frac{\partial \bar{H}}{\partial s} + \overline{\rho v}\frac{\partial \bar{H}}{\partial y} = \frac{1}{r}\frac{\partial}{\partial y}\left[\left(\frac{\mu}{Pr} + \frac{\mu_t}{Pr_t}\right) r \frac{\partial \bar{H}}{\partial y}\right] + \frac{1}{r}\frac{\partial}{\partial y}\left[\mu r\left(1 - \frac{1}{Pr}\right) + \mu_t r\left(1 - \frac{1}{Pr_t}\right)\right]\frac{\partial}{\partial y}\left(\frac{\bar{u}^2}{2}\right) \tag{9.e}$$

$$\bar{H}(0) = c_p T_w, \quad \bar{H}(\infty) = H_e, \quad \left.\frac{\partial \bar{H}}{\partial y}\right|_{y=\infty} = 0 \tag{9.f-h}$$

Under the approximation that both the molecular and turbulent Prandtl number are equal to 1 for gases, recalling the momentum and energy balances analogy, equations (9.a) and (9.e), for zero pressure gradients, and also between its

ISSN 2176-5480

boundary conditions, lead to the hypothesis that the total enthalpy is a function only of the longitudinal velocity component within the boundary layer (White, 1992). As a consequence, the total enthalpy can be obtained explicitly to vary linearly with the local velocity. Finally, making the assumption that the gas is calorically perfect and applying the boundary conditions, equations (9.b-d) and (9.f-h), one obtains equation (10) that is known as the Crocco-Busemann relation (White, 1992):

$$\bar{T} = T_w + (T_{aw} - T_w)\frac{\bar{u}}{u_e} - \frac{\bar{u}^2}{2c_p} \tag{10}$$

However, one may question the validity of this result for problems involving non-zero pressure gradients. It has been shown that for moderate values of the pressure gradient equation (10) still holds (White, 1992).

3. SOLUTION METHODOLOGY

3.1 Heat Conduction Problem

To proceed with the solution of the heat conduction problem along the Pitot tube, a hybrid numerical-analytical method known as the Generalized Integral Transform Technique (GITT) (Cotta, 1993; Cotta & Mikhailov, 1997) was employed. The main reasons for this choice were, first, the fact that the analytical task is performed just once and the numerical job is reduced to the solution of an ordinary differential system, making this hybrid approach well suited for iterative processes such as the one here implemented, and second the inherent numerical robustness of the solution methodologies for systems of initial value problems in comparison with direct numerical methods for partial differential equations.

The first step in this technique is the proposition of an eigenvalue problem, usually of the Sturm-Liouville type (Cotta, 1993; Cotta, 1998; Cotta & Mikhailov, 1997) which offers a basis for the eigenfunction expansion to be introduced. In this particular case, the adopted eigenvalue problem is presented in equations (11.a-c):

$$\frac{d}{dX}\left(k^*(X)A(X)\frac{d\Psi_i}{dX}\right) + w^*(X)A(X){\lambda_i}^2\Psi_i(X) = 0 \tag{11.a}$$

$$Bi_e\Psi_i(0) - k^*(0)\left.\frac{d\Psi_i}{dX}\right|_{X=0} = 0;\; Bi_L\Psi_i(1) + k^*(1)\left.\frac{d\Psi_i}{dX}\right|_{X=1} = 0 \tag{11.b,c}$$

It is evident that this boundary value problem is not readily solvable in terms of known orthogonal functions, in light of both the thermophysical properties and geometrical parameters variations along the longitudinal coordinate. However, it is here proposed that the eigenvalue problem itself be solved via the GITT. Therefore, a simpler eigenvalue problem is proposed in equations (12.a-c), which has a known exact solution in terms of trigonometric functions:

$$\frac{d^2\sigma_j}{dX^2} + {\omega_j}^2\sigma_j(X) = 0 \tag{12.a}$$

$$Bi_e\sigma_j(0) - k^*(0)\left.\frac{d\sigma_j}{dX}\right|_{X=0} = 0;\; Bi_L\sigma_j(1) + k^*(1)\left.\frac{d\sigma_j}{dX}\right|_{X=1} = 0 \tag{12.b,c}$$

With the solution to the auxiliary eigenvalue problem (12.a-c), a pair of transformation and inverse relations is developed and presented in equations (13.a,b):

$$\bar{\Psi}_{i,j} = \int_0^1 \sigma_j(X)\Psi_i(X)dX;\;\; \Psi_i(X) = \sum_{j=1}^{\infty}\bar{\Psi}_{i,j}\sigma_j(X) \tag{13.a,b}$$

The next step is to perform the integral transformation of the original eigenvalue problem (11.a-c) using the solution of the auxiliary problem (12.a-c) as the kernel. The result is an algebraic eigenvalue problem shown in equations (14.a-c) that is readily solvable using numerical techniques present in the *Mathematica v7.0* platform (Wolfram, 2005):

$$\left[\Lambda_{i,j}\right] + \lambda^2\left[\Gamma_{i,j}\right] = 0 \tag{14.a}$$

where,

$$\Lambda_{i,j} = \int_0^1 \sigma_i(X)\frac{d}{dX}\left(k^*(X)A(X)\frac{d\sigma_j}{dX}\right)\bar{\Psi}_{i,j};\;\; \Gamma_{i,j} = \int_0^1 \sigma_i(X)\sigma_j(X)w^*(X)A(X)\bar{\Psi}_{i,j} \tag{14.b,c}$$

Finally, after the normalization of the resulting eigenfunctions, it is possible to develop the transformation and inverse pair below for the temperature field in the solid:

$$\bar{\theta}_i(\tau) = \int_0^1 w^*(X)A(X)\widetilde{\Psi}_i(X)\theta_{av}(X,\tau)dX;\quad \theta_{av}(X,\tau) = \sum_{i=1}^{\infty}\widetilde{\Psi}_i(X)\bar{\theta}_i(\tau) \tag{15.a,b}$$

ISSN 2176-5480

Next, equation (8.a) is integral transformed using the solution of the eigenvalue problem (11.a-c) as the kernel. The solution is the infinite coupled system of ordinary differential equations shown below:

$$\frac{d\bar{\theta}_i}{d\tau} + \sum_{j=1}^{\infty} B_{i,j}\bar{\theta}_j(\tau) = \bar{g}_i(\tau), \qquad i = 1,2,3,\ldots \tag{16.a}$$

$$\bar{\theta}_i(0) = \bar{\theta}_{0_i} = \int_0^1 w^*(X)A(X)\widetilde{\Psi}_i(X)\frac{T_{av_0}(X)-T_{aw}}{T_{ref}-T_{aw}}dX \tag{16.b}$$

where,

$$B_{i,j} = {\lambda_i}^2\delta_{i,j} + \int_0^1 w^*(X)A(X)\widetilde{\Psi}_i(X)\widetilde{\Psi}_j(X)\frac{\Omega(X)L^2}{k_0}dX \tag{16.c}$$

$$\bar{g}_i(\tau) = \int_0^1 w^*(X)A(X)\widetilde{\Psi}_i(X)\frac{g_{av}(X,\tau)L^2}{k_0(T_{ref}-T_{aw})}dX \tag{16.d}$$

For computational purposes, this infinite system of equations is then truncated to a sufficiently large finite order. The linear transformed system is then analytically solved by employing the matrix exponential function, offering a very accurate and cost effective solution for the Pitot probe energy equation. The analytical solution of the transformed temperatures is then given by:

$$\left[\bar{\theta}_j(\tau)\right] = e^{-[B_{i,j}]\tau}\left[\bar{\theta}_{0_i}\right] + \int_0^\tau e^{-[B_{i,j}](\tau-\tau')}[\bar{g}_i(\tau')]d\tau' \tag{17}$$

Finally, through the inverse relation eq.(15.b0, one performs the analytical recovery of the final solution for the dimensionless temperature field in the solid.

3.2 Convection Problem

For the solution of the flow within the boundary layer that is formed around the Pitot tube it is proposed to use the well-known integral method of Karman-Pohlhausen (Schlichting, 1979; Kays & Crawford, 1980). It consists in approximating the velocity distribution along the direction perpendicular to the surface by a known function and relate this function to the boundary layer thickness through the boundary conditions. Then, the integral form of the boundary layer equations along the perpendicular direction is constructed, and upon substitution of the assumed velocity distribution, the resulting integrations lead to an ordinary differential equation for the boundary layer thickness. It is worthwhile recalling that with the adoption of the Crocco-Busemann relation there is no need to solve the energy equation in the fluid through the same approach. The working relations are then given in equations (18.a,b).

$$r\overline{\rho v}|_{y=\delta} = -\frac{\partial}{\partial s}\left(\int_0^\delta r\bar{\rho}\bar{u}dy\right) \tag{18.a}$$

$$\frac{d}{ds}\left(\int_0^\delta r\bar{\rho}\bar{u}(u_e-\bar{u})dy\right) = \frac{du_e}{ds}\left(\int_0^\delta r\bar{\rho}\bar{u}dy - \rho_e u_e\int_0^\delta rdy\right) + r_o\tau_w \tag{18.b}$$

For the laminar portion of the boundary layer, the most usual third order polynomial profile is proposed, with coefficients given by substitution in the boundary conditions of equations (19.a-d), while for the turbulent portion of the flow, the 1/7 power profile presented in equation (20) is applied.

$$u(s,0) = 0; \quad \rho_e u_e\frac{du_e}{ds} + \frac{1}{r}\frac{\partial}{\partial y}\left(\mu r\frac{\partial u}{\partial y}\right)\Big|_{y=0} = 0 \tag{19.a,b}$$

$$u(s,\delta) = u_e; \quad \frac{\partial u}{\partial y}\Big|_{y=\delta} = 0 \tag{19.c,d}$$

$$u^+ = 8.74y^{+1/7} \tag{20}$$

3.3 Conjugated Problem

In order to avoid algorithm complications in light of the different methods and different coordinates systems employed for each domain, an iterative process was implemented as displayed in the flowchart of figure 8. The convergence of such procedure has proved to be quite fast, for the full range of situations here simulated. Simultaneous solution of the conjugated problem equations is also feasible, but was not found to be the most efficient computationally in the present application.

ISSN 2176-5480

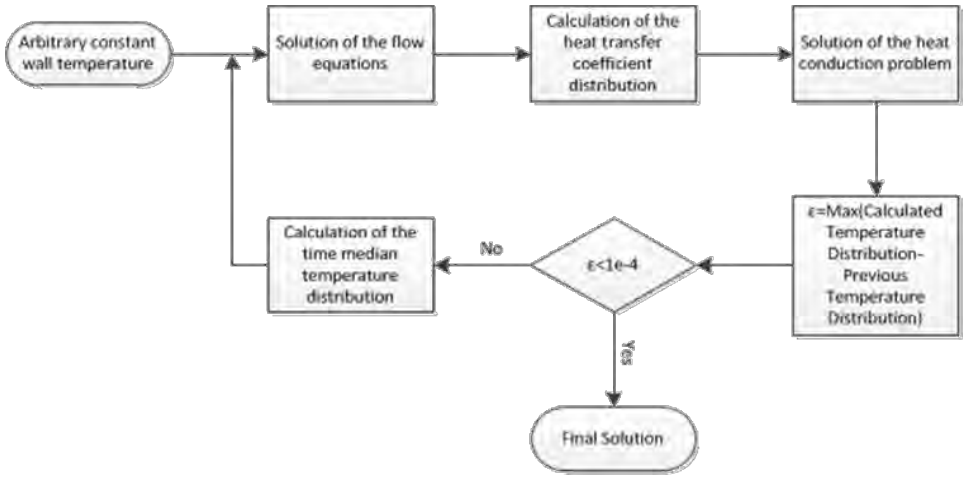

Figure 8. Flowchart of the iterative process implemented in the solution of the conjugated problem.

4. RESULTS AND DISCUSSION

4.1 Validation for Incompressible Flow: Wind Tunnel Experiments

In a recent work, (Souza et al., 2011) conducted experiments in a metrological wind tunnel available at INMETRO (Instituto Nacional de Metrologia, Padronização e Qualidade Industrial), in order to validate the simple heat conduction model then proposed for the Pitot probe. Some of the data generated in that experiment has been used in the present work to offer a validation of the present conjugated convection-conduction model for incompressible flow conditions. The measurements available include the LDA velocity field for the flow around the Pitot tube and the transient temperature distributions over the Pitot tube surface generated by infrared thermography, as illustrated in figure 9. The model developed in section **Error! Reference source not found.** is here confronted with the experimental results generated by (Souza et al., 2011). Figure 10 shows the comparison between the steady state results obtained with the simulation and the experiments, for the temperature distribution along the length of the probe, since the tip (x=0) up to the end of the support region (x=L). One may conclude that the adherence between the two sets of results is quite satisfactory, deviating only at the end of the support region, basically due to the heat losses at the end of the Pitot tube support that were not taken into account.

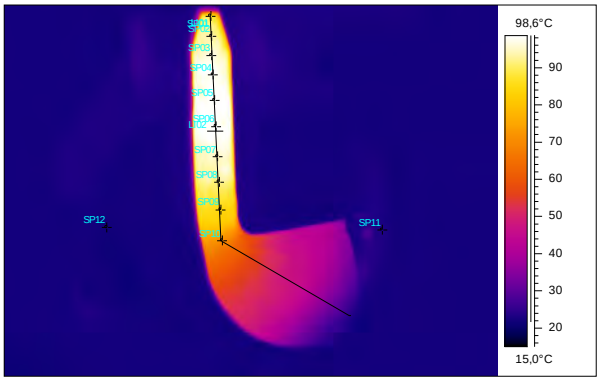

Figure 3. Illustration of the infrared thermography results from the wind tunnel experiments (9.98 m/s, 68 V and 0.69 A in the resistor)

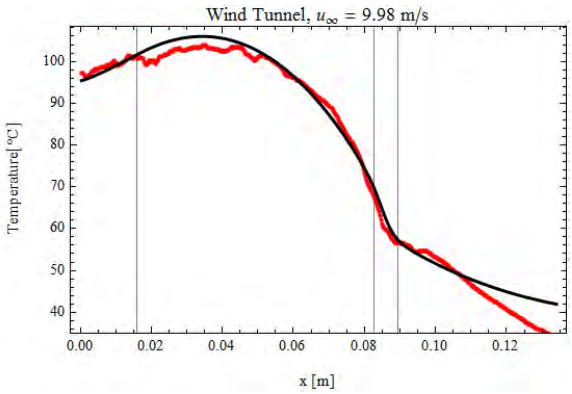

Figure 4. Comparison between the steady state temperature fields: experimental, in red, and simulated, in black.

As for the transient behavior, starting from the unheated probe in thermal equilibrium with the free stream air, and suddenly turning on the heating system, the measurements taken by infrared thermography are compared in figure 11 with the simulation results for several positions along the longitudinal coordinate. The agreement between the two sets of results is again excellent, giving confidence that the conjugated model is perfectly capable of accurately describing the transient behavior of the temperature field along the Pitot tube. However, if the porcelain electrical insulation is not accounted for in the effective thermophysical properties, particularly in the local thermal capacity, significant deviations between experimental and theoretical results are observed, as discussed in (Souza et al., 2011; Souza et al., 2012).

ISSN 2176-5480

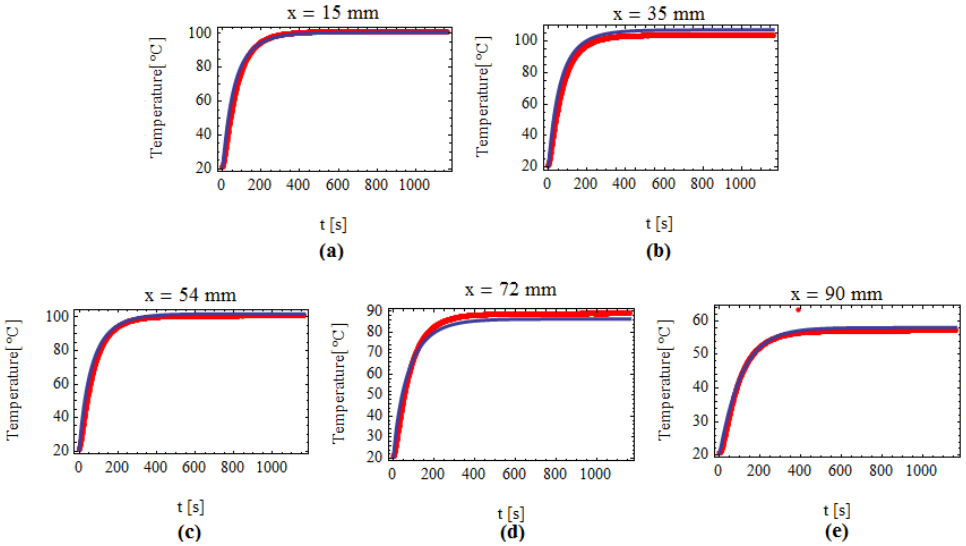

Figure 5. Comparison between the time evolution of measured (red) and simulated (blue) temperatures at different positions along the Pitot probe length, for the wind tunnel experiments.

4.2 Validation for Compressible Flow: Flight Tests

In another recent work (Souza et al., 2012), flight tests were conducted in a A-4 Skyhawk aircraft of the VF-1 Squadron, in the Brazilian Aero-Naval Base, at São Pedro d´Aldeia, Rio de Janeiro, in order to determine the thermal behavior of an instrumented Pitot tube under actual flight conditions and thus validate the models developed for these compressible flow situations. In order to generate abrupt transient variations, the A4 pilot was required to repeatedly turn on and off the Pitot thermal protection system, thus allowing for the observation of the thermal response of the probe to sudden heat transfer perturbations. Two flights were here selected for analysis, the first with a Mach number of 0.5 and at 10000 ft of altitude, and the second one with a Mach number of 0.51 and at 15000 ft of altitude.

Figure 12 shows the predicted transient behavior of the Pitot probe temperature at a point located 80 mm from the stagnation point, accounting for the influence of the porcelain's heat capacity in the time response. Both the classical lumping (red curves) and improved lumped (black curves) procedures have been included in this comparison. The experimental thermocouple readings are plotted in blue, while the measured external air temperature is shown in green lines. It can be noticed that the model slightly under-predicts the time necessary to reach steady state after each switching cycle at the lower altitude, with a closer agreement in the higher altitude flight. Another worthy observation is that for the 10000 ft flight the two lumping approaches differ more noticeably, with the present improved lumped approach yielding better results. This is due to the fact that the heat transfer coefficients are higher at the lower altitude flight, i.e., higher velocities and denser air, and thus the Biot numbers tend to be higher in this case, which favors the use of the improved lumped analysis for higher accuracy.

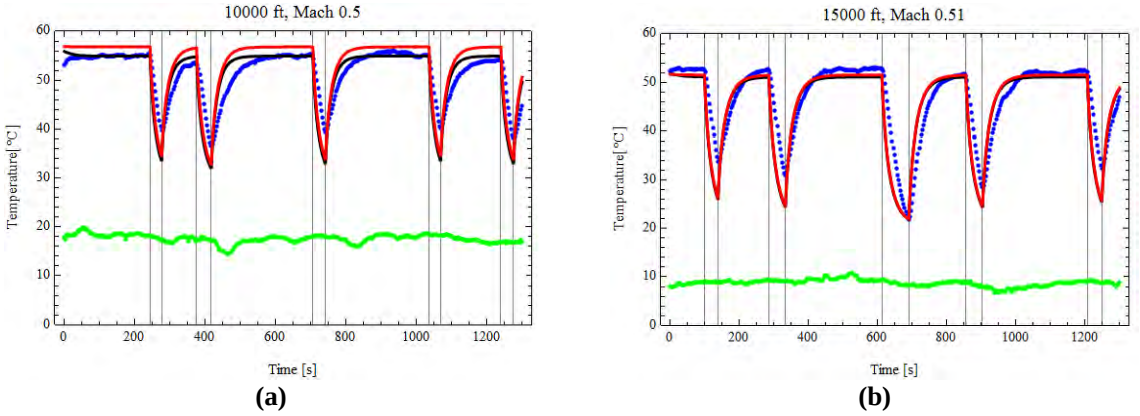

Figure 6. Time evolution of the temperature at the surface of the Pitot distant 80 mm from the stagnation point, considering the porcelain influence, with improve lumped, in black, with classical lumped, in red, and with experimental results, in blue: (a) flight at 10000 ft and Mach 0.5; (b) flight at 15000 ft and Mach 0.51.

ISSN 2176-5480

Steady state theoretical results for the A4 flights have also been analyzed, by comparing the simple thermal model using correlations for the external heat transfer coefficient (Souza et al., 2011), against the complete conjugated problem here proposed. Figure 13 shows that the uncoupled model (in red) overestimates the probe surface temperatures at the stagnation and tip regions in both flight situations, to within 5ºC in comparison to the full conjugated model (in black). This result reconfirms the importance of taking into account the mutual influence between the solid and the fluid and the need for a more complete conjugated model to more accurately describe the thermal behavior of the Pitot tube under critical conditions.

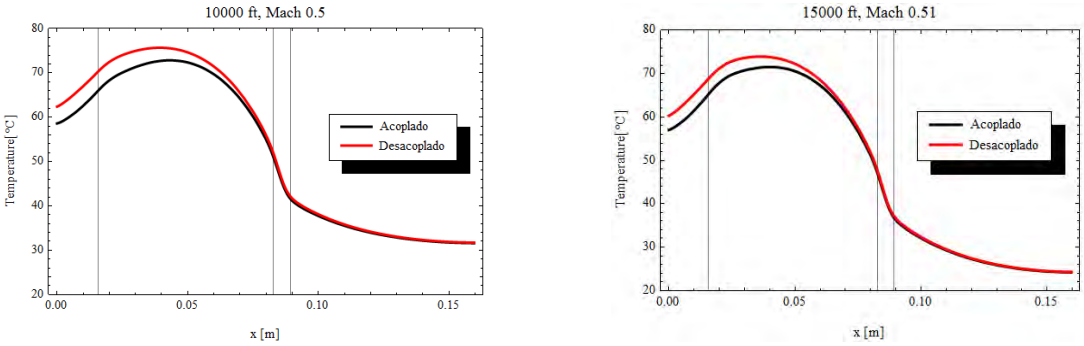

Figure 7. Temperature distribution along longitudinal position in steady state:
(a) flight at 10000 ft and Mach 0.5; (b) flight at 15000 ft and Mach 0.51.

4.3 Design Parametric Studies

Avoiding ice accretion at the stagnation region is critical for the well functioning of the Pitot tube. Thus, parametric studies for the design of anti-icing systems are aimed at turning the sensor more reliable under ice formation conditions, for instance by trying to raise the surface temperatures at this region. Just as an example of parametric studies that are allowed for by the modeling here advanced, two modifications in the design of the PH-510 are analyzed: a linear distribution of heat generation by Joule effect with the maximum near the stagnation point, instead of the more usual uniform heat generation pattern, and the elimination of the cone portion making the probe totally cylindrical and thus allowing to bring the thermal protection system forward towards the probe tip, generating heat closer to the stagnation region.

The first proposition is implemented by maintaining the total power dissipation in the resistor and just redistributing it along the probe length. A linear distribution is first proposed and with a fairly small deviation from the uniform distribution, as shown in figure 14. Figure 15 presents the temperature results at the stagnation point for both flight conditions of the previous subsection, where even though the change in the distribution is small, the effect is already noticeable. In this case, an increase of about 1.5 ºC in the stagnation point temperature was reached.

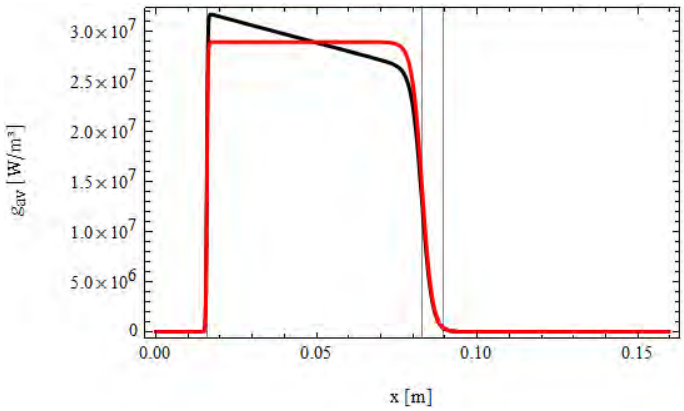

Figure 8. Energy generation by Joule effect distribution along the longitudinal direction:
modified linear distribution, in black, uniform distribution, in red.

ISSN 2176-5480

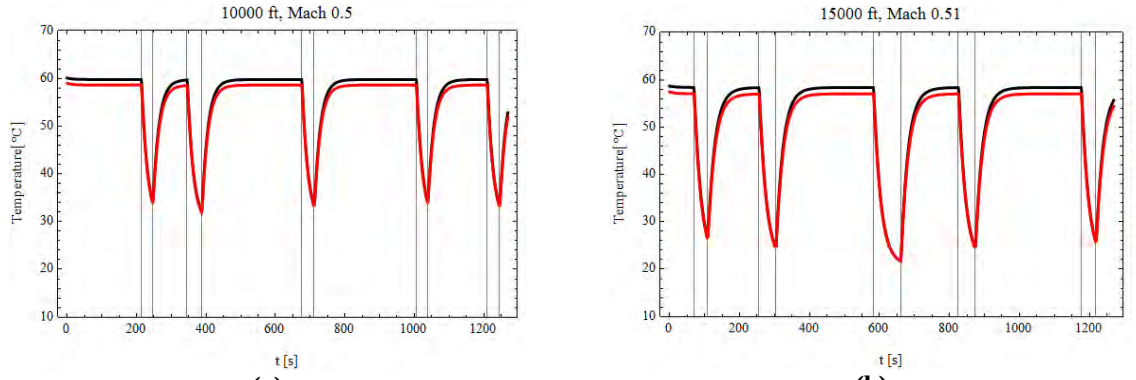

(a) **(b)**

Figure 9. Comparison between the temperature at the stagnation point obtained with a linear power density distribution, in black, and with an uniform power density distribution, in red:
(a) flight at 10000 ft and Mach 0.5; (b) flight at 15000 ft and Mach 0.51.

As for the second modification, adopting a straight cylindrical probe, the results for the stagnation point temperature are shown in Figure 16. The relative change in the temperature at the stagnation point when comparing the original PH-510 with the modified one, was of about 26%, which is indeed a more impressive improvement, after a straightforward modification in the probe concept.

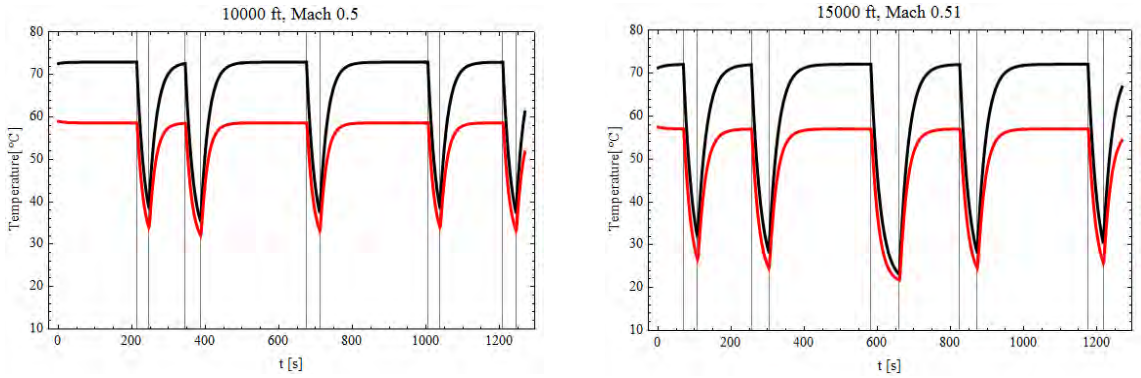

(a) **(b)**

Figure 10. Time evolution of the stagnation point evolution for a totally cylindrical probe, in black, and for the original geometry of the PH-510 used in the validation of the model:
(a) flight at 10000 ft and Mach 0.5; (b) flight at 15000 ft and Mach 0.51.

5. CONCLUSIONS

The results here obtained and critically compared to both incompressible and compressible flow experiments, demonstrated that the developed conjugated model and associated solution methodology, is capable of accurately predicting the transient thermal behavior of aeronautical Pitot tubes with anti-icing systems, in both controlled laboratory wind tunnel runs and in real airplane flights.

Concerning the parametric studies conducted in the present work, the change in the power density profile was shown to have a proportional effect on the temperature at the stagnation region. Also, a simple modification in the geometry, by considering a straight cylindrical probe, allowing the placement of the thermal protection system further forward towards the tip, proved to offer a significant improvement of the anti-icing system. The constructed model may be a valuable tool in the thermal design improvement of anti-icing systems for aeronautical velocity sensors.

6. ACKNOWLEDGEMENTS

The authors are indebted to the VF-1 Squadron, Brazilian Aero-Naval Base, São Pedro d´Aldeia, Rio de Janeiro, for providing the Pitot tubes here employed and sponsoring the A4 flight tests. The financial support of CNPq and FAPERJ is also acknowledged. This work is dedicated to the 228 victims of the AF447 flight and their families.

7. REFERENCES

Caliskan; F., Aykan, R., Hajiyev, C., 2008, Aircraft Icing Detection, Identification, and Reconfigurable Control Based on Kalman Filtering and Neural Networks, J. of Aerospace Engineering, v. 21, no. 2, pp.51-60.

Cebeci, T., Cousteix, J., 2005, Modeling and Computation of Boundary Layer Flows, 2nd edition, Springer.

Cotta, R.M., 1990, Hybrid numerical-analytical approach to nonlinear diffusion problems, Num. Heat Transfer, Part B, vol. 127, pp.217-226.

Cotta, R.M., 1993, Integral Transforms in Computational Heat and Fluid Flow, CRC Press.

Cotta, R.M., 1994, Benchmark results in computational heat and fluid flow: the integral transform method, Int. J. Heat & Mass Transfer (Invited paper), v.37, Suppl. 1, pp. 381-394.

Cotta, R.M., Mikhailov, M.D., 1997, Heat Conduction: Lumped Analysis, Integral Transforms, Symbolic Computation, Wiley-Interscience, Chichester, UK.

Cotta, R.M., 1998, The Integral Transform Method in Thermal and Fluids Sciences and Engineering, Begell House.

Cotta, R.M., Mikhailov, M.D., 2006, Hybrid methods and symbolic computations, in: Handbook of Numerical Heat Transfer, 2nd edition, Chapter 16, Eds. W.J. Minkowycz, E.M. Sparrow, and J.Y. Murthy, John Wiley, New York.

Gent, R. W., Dart, N. P., Cansdale, J. T., 2000, Aircraft Icing, Phil. Trans. R. Soc. Lond. A, v. 358, pp.2873-2911.

Heinrich, A., Ross, R., Zumwalt, G., Provorse, J., Padmanabhan, V., Thompson, J., Riley, J., 1991, Aircraft Icing Handbook, vol. 2., chapter III, FAA Technical Center.

Kays, W.M., Crawford, M.E., 1980, Convective Heat and Mass Transfer, 2nd edition, McGraw Hill, New York.

Lisboa, K.M., Souza, J.R.B., Cotta, R.M., Naveira-Cotta, C.P., 2012, Transient Conjugated Heat Transfer in External Compressible Laminar Flow over Plates with Internal Heat Generation, Proc. of the 7th CONEM - Congresso Nacional de Engenharia Mecânica, São Luis, MA, Brazil.

Luikov, A.V., Aleksashenko, V.A., and Aleksashenko, A.A., 1971, Analytical Methods of Solution of Conjugated Problems in Convective Heat Transfer, Int. J. Heat and Mass Transfer, Vol. 14, pp. 1047-1056.

Luikov, A.V., 1974, Conjugate Convective Heat Transfer Problems, *Int. Journal of Heat and Mass Transfer*, v. 17, no.2, pp. 257-265.

Mayall, M.C.M., 2003, Análise de Aquecimento Aerodinâmico em Micro-Satélite Durante Reentrada Atmosférica, M.Sc., PEM, COPPE-UFRJ.

Mikhailov, M. D., Ozisik, M. N., 1984, Unified Analysis and Solution of Heat and Mass Diffusion, John Wiley.

Osizik, M.N., 1985, Heat Transfer: A Basic Approach, McGraw-Hill, New York.

Ozisik, M.N., 1993, Heat Conduction, 2nd edition, John Wiley and Sons, New York, NY, EUA.

Perelman, Y.L., 1961, On Conjugate Problems of Heat Transfer, Int. J. Heat and Mass Transfer, Vol. 3, pp.293-303.

Schlichting, H., 1979, Boundary Layer Theory, 7th edition, McGraw-Hill, New York.

Schlichting, H., Truckenbrodt, E., 1979, Aerodynamics of the Airplane, 1st edition, McGraw-Hill, New York.

Souza, J.B.R., Zotin, J.L.Z., Loureiro, J.B.R., Naveira-Cotta, C.P., Silva Freire, A.P., Cotta, R.M., 2011, Conjugated Heat Transfer Analysis of Heated Pitot Tubes: Wind Tunnel Experiments, Infrared Thermography and Lumped-Differential Modeling, 21st COBEM- Congresso Brasileiro de Engenharia Mecânica, 2011, Natal, Brazil.

Souza, J.B.R., Lisboa, K.M., Cerqueira, I.G., Naveira-Cotta, C.P., Cotta, R.M., Zotin, J.L.Z., 2012, Conjugated Heat Transfer Models for Heated Aeronautical Pitot Tubes: Experimental Validation with A-4 Skyhawk Flight Tests, 14th ENCIT – Brazilian Congress of Thermal Sciences and Engineering, 2012, Rio de Janeiro, Brazil.

Tong, Z.M., Hu, Y.H., 2009, Convective Heat Transfer and Flow Resistance Characteristics of Various Types of Elliptical Tubes, Proc. of the Int. Conf. on Energy and Environment Technology, IEEE.

White, F.M., Christoph, G.H., 1972, A Simple Theory for the Two-Dimensional Compressible Turbulent Boundary Layer, ASME Trans. J. Basic Eng., vol. 94, Ser. D, pp. 636-642.

White, F. M., 1992, Viscous Fluid Flow, McGraw-Hill.

Wolfram, S., 2005, The *Mathematica* Book, Cambridge-Wolfram Media.

8. RESPONSIBILITY NOTICE

The authors are the only responsible for the printed material included in this paper.